ELSEVIER

Biochimica et Biophysica Acta 1231 (1995) 98–110

BBA Biochimica et Biophysica Acta

Kinetics of ATP hydrolysis by the F_1-ATPase from *Bacillus* PS3: a reappraisal of the effects of ATP and Mg^{2+}

Stéphane Pezennec [a,*], Gérard Berger [a], Sandra Andrianambinintsoa [a], Nicolas Radziszewski [a], Guy Girault [a], Jean Michel Galmiche [a], Edmund Bäuerlein [b]

[a] *Section de Bioénergétique, Département de Biologie Cellulaire et Moléculaire, CEA Centre d'Etudes de Saclay, 91191 Gif sur Yvette Cedex, France*
[b] *Max-Planck-Institut für Biochemie, 82152 Martinsried, Germany*

Received 25 October 1994; revised 7 April 1995; accepted 20 April 1995

Abstract

ATPase activity of the F_1-ATPase from the thermophilic *Bacillus* PS3 (TF_1) was measured as a function of ATP concentration at three different magnesium ion concentrations. A high-performance chromatographic method was used to determine directly ADP concentration in the reaction medium and to measure the steady-state rate of its appearance. Multiphasic curves of ATPase activity versus ATP concentration were obtained, with a first saturating rate mode at low ATP concentrations, a higher rate mode which became predominant at ATP concentrations depending on magnesium concentration, and a marked inhibition of ATP hydrolysis at high ATP concentrations. These curves could be simulated with equivalent residual error either by assuming that the ATP-magnesium chelate is the substrate of the enzyme, free magnesium being an inhibitor, or that free ATP is the substrate, free magnesium being an essential activator. In both cases, the observed hydrolysis rate was assumed to be the sum of two independent rates with different kinetic parameters, as would be the case for an enzyme with functionally heterogeneous and independent catalytic sites. Cross-checking of the different series of kinetic parameters with the binding affinity of TF_1 for ATP, measured by a high-performance chromatographic method, is in favour of a model in which the hydrolysis rate is determined by the concentration of free ATP, free magnesium being an essential activator.

Keywords: HPLC; ATPase, H^+-; Adenine nucleotide; Binding site; Kinetics; ATP hydrolysis

1. Introduction

F-type ATP synthases are a family of membrane-bound enzymes which utilise the electrochemical potential of a proton gradient produced by redox chains in all energy-transducing membranes; they catalyse the reversible phosphorylation of adenosine diphosphate to adenosine triphosphate. They are found in the bacterial plasma membrane, the chloroplast thylakoid membrane, and the inner mitochondrial membrane. F-type ATP synthases from *Escherichia coli*, chloroplasts, mitochondria, and from the thermophilic *Bacillus* PS3 have been studied most intensively. The high structural homology among F-type ATP synthases from various sources allowed a common structural scheme to be proposed [1–3].

The F-type ATP synthases are composed of two distinct moieties. F_1, which is extrinsic to the membrane and catalyses the phosphorylation reaction, can be separated from its membrane-spanning counterpart F_0, which mediates proton translocation. F_1 then constitutes a stable water-soluble ATP-hydrolase (ATPase). Three-dimensional structures have been recently obtained for mitochondrial F_1 [4,5]. One of them [5] provides an asymmetric model for the nucleotide-binding sites. The way in which the energy is transmitted through F_0 to the catalytic sites on F_1 still remains unknown. Many structural and functional investigations about nucleotide binding and ATP hydrolysis have been performed with the isolated F_1-ATPase.

It is generally accepted that F_1 bears six nucleotide binding sites [6–8]. Three of them exchange bound adenine nucleotides with nucleotides of the medium [6,9,10]. The three other sites exchange bound nucleotides very slowly, if at all, with nucleotides of the medium [9,10]; their functional role is still an open question [11–14]. The

Abbreviations: TF_1, CF_1 and MF_1, the soluble catalytic moiety of the F-type ATP-synthase complex from *Bacillus* PS3, chloroplasts and mitochondria, respectively; CF_1-ϵ, CF_1 depleted of its ϵ subunit; Tris, 2-amino-2-hydroxymethylpropane-1,3-diol; HPLC, high performance liquid chromatography; TNP-ATP, 2′,3′-*O*-(2,4,6-trinitrophenyl)-ATP.

* Corresponding author. E-mail: pezennec@dsvidf.cea.fr. Fax: +33 1 69088717.

SSDI 0005-2728(95)00071-2

correspondence between the ability to exchange bound nucleotides and catalytic properties is not definitely established: indeed, one slowly exchangeable ADP bound to the enzyme from *Bacillus* PS3 (TF_1)[1] [15], CF_1 [16] and MF_1 [17] appears to be bound at a catalytic site.

Numerous studies have been performed about ATP hydrolysis catalysed by F_1 from various sources. Considering the dependence of ATPase activity on the presence of a divalent cation and the ability of nucleotides to chelate divalent cations with high affinity [18], most of the data about the effects of divalent cations on catalytic properties of F_1 were interpreted by a model, nowadays generally accepted, involving hydrolysis of the nucleotide-metal chelate and inhibition of the hydrolytic activity of the enzyme by free magnesium and by free ATP [19–22].

Recently the influence of total magnesium ion concentration on the hydrolytic activity of chloroplast F_1-ATPase depleted of its ϵ subunit (CF_1-ϵ) and ATP binding were investigated [23]. Confrontation between binding results and kinetic data and analysis of inhibitory effects of sodium ions were found to need the hypothesis that free ATP is the nucleotide species that is bound to, and hydrolysed by magnesium-activated CF_1-ϵ. These results motivated further study of the mechanism of ATP hydrolysis by another F_1-ATPase, TF_1.

TF_1, the ATPase from the thermophilic *Bacillus* strain PS3, is a fully active ATPase, i.e., it exhibits maximum ATPase activity without requirement for any activation procedure. It is also, as far as we know, the only soluble ATPase which is free of bound adenine nucleotides [24] when isolated by the procedure already described [25]. In the present work, we probed the hydrolytic properties of TF_1 at various total magnesium ion concentrations. ATPase activities were measured at 37°C by anion-exchange HPLC of adenine nucleotide species in the reaction medium [26]. TF_1 was shown to exhibit multiphasic ATPase activity patterns which were strongly modulated by total magnesium ion concentration. Theoretical treatment of the kinetic data was performed, using simple steady-state assumptions, postulating two possible hydrolysis mechanisms. In an attempt to discriminate between these mechanisms we also measured binding affinities of TF_1 for adenine nucleotides. The results are discussed with respect to available data about TF_1 and the catalytic mechanism of F_1-ATPases. It is concluded that kinetic data alone cannot discriminate between the two mechanisms, but that their confrontation with binding data does not support the commonly accepted hypothesis that ATP-Mg is the substrate of F_1-ATPases.

2. Materials and methods

2.1. Chemicals

Ammonium sulfate and magnesium sulfate of analytical grade were purchased from Merck. Tris, ADP (sodium salt) and ATP (disodium salt) were from Sigma. Potassium dihydrogenophosphate and sodium chloride were purchased from Prolabo.

2.2. HPLC apparatus

High-performance liquid chromatography was performed with a Waters apparatus consisting of two Model 510 pumps, controlled by a Model 660 solvent programmer when a gradient was performed, a U6K injector with a 2 ml sample loop, and a photometric detector Model Lambda Max 481 (for protein purification and nucleotide analysis), or Model 490 E (for binding studies).

2.3. Materials

Thermophilic bacterium PS3 was cultivated at 65°C in a 200 l fermentor, essentially as described [25], except that 2.5% (w/v) glucose was added into the growth medium. The presence of glucose in the medium shortened the lag phase of bacterial growth and significantly increased the yield in biomass. During the growth, regulation of the pH to 7.0 using NaOH was necessary to avoid the pH drop induced by consumption of glucose by bacteria.

Preparation of washed membranes, chloroform extraction, and purification of TF_1 were performed as described [25]. In the final steps, the purification procedure described for CF_1 [27] was applied: the final size exclusion chromatography on Sepharose CL 6B [25] was replaced by anion-exchange HPLC on a Waters Protein PAK DEAE 5PW semi-preparative column (2.15 × 15 cm) equilibrated with a buffer containing 50 mM Tris-H_2SO_4, 0.1 M $(NH_4)_2SO_4$ (pH 8.0). TF_1 was eluted at room temperature by a linear gradient of $(NH_4)_2SO_4$ concentration from 0.1 M to 1 M in 1 h. The flow rate was 6 ml min^{-1}. Proteins were detected by UV absorption at 280 nm. Purity of TF_1 at the column exit was checked by measuring the ratio of fluorescence emission at 310 nm and 340 nm upon excitation at 280 nm. TF_1 was precipitated with $(NH_4)_2SO_4$ at 70% saturation. Depending on the purity of the protein obtained, an additional size exclusion HPLC step was performed, after dissolution of the precipitate and extensive dialysis against 150 mM Tris-H_2SO_4 (pH 8.0), on a TSK 4000 SW column (0.75 × 30 cm) equilibrated with the same buffer, at a flow rate of 1 ml min^{-1}. TF_1 was stored as an ammonium sulfate precipitate at 4°C, and extensively dialysed before use.

Protein concentrations were measured [28] with the BioRad protein assay, using bovine serum albumin as a standard.

2.4. HPLC analysis of nucleotides: determination of endogenous nucleotides and ATPase activity

Adenine nucleotide analysis was performed as previously described [26] by isocratic elution on an anion-ex-

change TSK DEAE 2SW column (0.46 × 25 cm) with 0.1 M KH_2PO_4, 0.25 M NaCl, at a flow rate of 1.5 ml min^{-1}. Nucleotides were detected in the effluent by UV absorption at 260 nm. Concentrations of separated nucleotides were measured by the height of the absorption peak after calibration in the same conditions. ATP and ADP concentrations in standard solutions were calculated assuming a molar absorption coefficient at 260 nm of $1.54 \cdot 10^4$ M^{-1} cm^{-1}.

Determination of endogenous nucleotides

TF_1 (20 μl, approx. 20 mg ml^{-1}) was denatured by the addition of 20 μl of 2 M HCl. The mixture was kept in an ice-bath for 5 min. 20 μl of 2 M NaOH and 140 μl of distilled water were then added prior to centrifugation at 10000 × *g* for 10 min. The supernatant fraction was immediately separated from the pellet in order to avoid any subsequent nucleotide binding to the precipitated protein, and used for anion-exchange HPLC determination. The stoichiometry of endogenous nucleotides was calculated assuming a molecular weight of 385700 for TF_1, according to the genes sequences published [29].

Measurement of ATPase activity

ATPase activities were measured at 37°C in a buffer containing 50 mM Tris-H_2SO_4 (pH 8.0), and the indicated concentration of $MgSO_4$ (either 0.2 mM, 1 mM or 2.5 mM), with ATP concentrations ranging between 2 μM and 5 mM. ATP hydrolysis, following incubation of the medium (0.5 ml) for several minutes at 37°C, was initiated by the addition of TF_1 to a final concentration close to 0.4 nM. This concentration was chosen in order to observe a linear rate of ATP hydrolysis for several minutes over the whole range of ATP concentrations studied (see Results). Aliquots of the reaction medium were withdrawn every 2.5 min and injected into the anion-exchange column. Spontaneous ATP hydrolysis in the reaction medium without protein and ADP concentration at zero time (before addition of the enzyme) were systematically measured by the same method; the former was found to be negligible. Initial ADP concentration in the reaction medium (due to contamination of ATP) was subtracted from the data. The activity of TF_1 was estimated by least-squares linear regression analysis of ADP produced versus time. ATPase activity was expressed as a specific activity. Quantitative treatment of kinetic data is described in detail under Results.

2.5. Measurement of adenine nucleotide binding to TF_1 by HPLC

Binding studies were performed using the chromatographic method first described by Hummel and Dreyer [30]. This method has been applied to the investigation of nucleotide binding sites of CF_1 by size exclusion [8] and by anion-exchange HPLC [23,31].

The principle of the method is the following: the column is equilibrated with a constant concentration of the ligand under study. As the protein is injected into the column, it binds a quantity of ligand which is proportional to the amount of protein injected. The bound ligand migrates together with the protein, while a trough in the chromatographic profile migrates with the ligand retention and generates a negative peak. The local deficit of ligand generating the trough is due to the sum of (1) the lack of ligand in the volume injected and (2) the amount of ligand bound to the protein at the moment of injection. According to the multiple equilibrium theory [32], the average number of moles of ligand bound per mole of protein is determined by the free ligand concentration and by the affinity constants of the different independent binding sites. The area of the negative peak is thus linearly related to the amount of bound ligand. Repetitive injections of the protein mixed with known amounts of added ligand allow an internal calibration of the method.

This method is limited to equilibria which are reached rapidly with respect to the time scale of the chromatographic separation. Since the complex is always in equilibrium with a constant concentration of ligand, no perturbation of the binding equilibrium occurs. As compared to binding measurements with centrifuge Sephadex column [33], this method allows large dissociation constants to be measured.

For studies of nucleotide binding to TF_1, the protein was dialysed overnight against a buffer containing 50 mM Tris-H_2SO_4 (pH 8.0), and 1 mM $MgSO_4$. The column was equilibrated at room temperature with the same buffer but containing different concentrations of the nucleotide, either ADP or ATP, at a flow rate of 1.2 ml min^{-1}. Two HPLC columns were used: a size exclusion column TSK 2000 SW (0.75 × 30 cm) for ADP binding, and an anion-exchange column TSK DEAE 2SW (0.46 × 25 cm) for ADP and ATP binding. Nucleotide concentration in the effluent was measured by the absorption at 260 nm. For all nucleotide concentrations, several injections were performed, each one immediately after mixing TF_1 with a known amount of nucleotide for internal calibration. The area of the absorption peak at 260 nm corresponding to the nucleotide under study was plotted versus excess of nucleotide, and linear regression was performed. The intersect of the resulting straight line with the abscissa axis gave the average number of moles of bound nucleotide per mole of TF_1. Binding models are described under Results.

2.6. Fitting of the data

Kinetic models and nucleotide binding models were fitted to the data by a non-linear least-squares procedure using the iterative Levenberg-Marquardt method.

3. Results and data analysis

3.1. Kinetic analysis of ATP hydrolysis catalysed by TF_1

Steady-state rate of ATP hydrolysis

Typical chromatograms and time-course patterns of ADP production are shown in Fig. 1. As already outlined [23,26], isocratic anion-exchange HPLC enabled us to separate ADP and ATP with a resolution larger than 2 (Fig. 1A) and to measure, in a direct and reliable manner, the steady-state rate of appearance of ADP. This direct determination of product concentration in the reaction medium avoids the use of a complex enzymatic regenerating system [34], in which phosphoenolpyruvate forms a complex with Mg^{2+} [35] and thus reduces its free concentration.

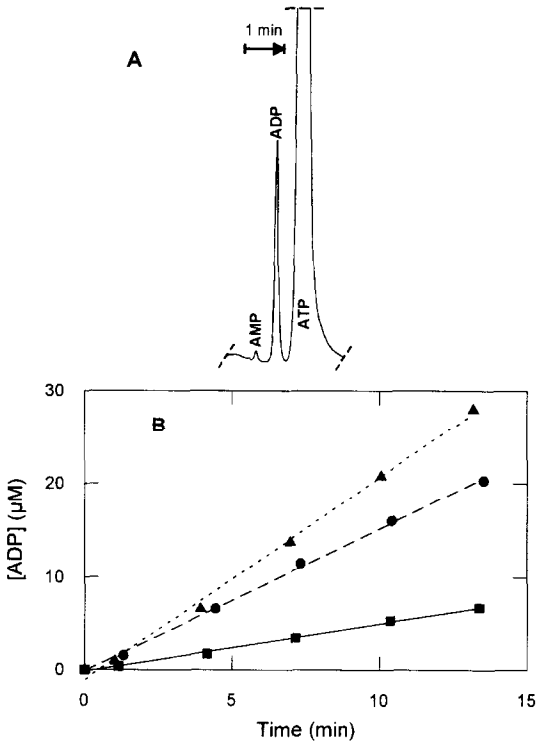

Fig. 1. Measurement by anion-exchange HPLC of the steady-state rate of ATP hydrolysis catalysed by TF_1. ATPase activity was measured at 37°C in a buffer containing 50 mM Tris-H_2SO_4 (pH 8.0), and either 0.2 mM, 1.0 mM or 2.5 mM $MgSO_4$, as a function of total ATP concentration ($[ATP_t]$). ATP hydrolysis was initiated following incubation of the reaction medium (0.5 ml) for several minutes at 37°C by addition of native TF_1 to a final concentration of approx. 0.4 nM. Aliquots of the reaction medium were withdrawn every 2.5 min and injected into an anion-exchange HPLC column (TSK DEAE 2SW 0.46×25 cm). Produced ADP was separated from ATP by isocratic elution with 0.1 M KH_2PO_4, 0.25 M NaCl (pH 4.3) at a flow rate of 1.5 ml min^{-1}, and its concentration was measured by the height of the UV absorption peak at 260 nm after calibration in the same conditions, assuming a molar absorption coefficient of $1.54 \cdot 10^4$ M^{-1} cm^{-1}. (A) Typical chromatogram of nucleotide separation. Injection of an aliquot (15 μl) of the reaction medium was performed during ATP hydrolysis by TF_1; in this example, total ATP concentration was 1 mM, total Mg^{2+} concentration was 1 mM. Average retention times of AMP, ADP and ATP were respectively 2.9 min, 3.4 min and 4 min. (B) Typical time-courses of ADP production at 0.2 mM total Mg^{2+}; in these examples, ATP concentration was 0.12 mM (squares), 0.35 mM (circles) and 0.7 mM (triangles). ADP concentrations at zero time (due to contamination of ATP) were systematically measured and subtracted from all the measurements. ATPase activities were taken as the slopes of the straight lines obtained by linear regression.

In the major part of the experimental domain, this steady-state rate was constant from zero time up to at least approx. 15 min (Fig. 1B). Linearity of ATP hydrolysis versus time also excludes any significant influence of competitive inhibition by produced ADP under these conditions.

Rate of ATP hydrolysis as a function of total ATP concentration: multiphasic pattern

The ATPase activity profiles as a function of total ATP concentration ($[ATP_t]$) at three different total Mg^{2+} concentrations ($[Mg_t^{2+}]$) are shown in Fig. 2. $[Mg_t^{2+}]$ strongly modulates the kinetics. For the studied values of $[Mg_t^{2+}]$, the activity profiles were complicated functions of $[ATP_t]$. Even though the three profiles were neither superimposable nor homothetic, they could be analysed in terms of homologous phases.

Three distinct phases can be defined in the plots. Phase I is only apparent at 1 mM and 2.5 mM total Mg^{2+} (Fig. 2B,C). It consists in the initial part of the plots, characterised by a saturating profile, curved downwards and by low levels of specific activity. At 2.5 mM total Mg^{2+}, the slow rate mode exhibited in this first phase is predominant in a larger range of $[ATP_t]$ than at 1 mM total Mg^{2+}, but activity levels are comparable. At higher $[ATP_t]$, beyond a marked transition with considerable acceleration of the hydrolysis, phase II has also a saturating profile, curved downwards and displays a high rate mode of hydrolysis. At 0.2 mM and 1 mM total Mg^{2+}, the specific activity reaches a maximum (Fig. 2A,B). Then, phase III is characterised by the inhibition of the hydrolytic activity at high $[ATP_t]$. Although phase III was not observed at 2.5 mM total Mg^{2+} (Fig. 2C), inhibition at high total ATP concentration is probably a constant feature of the hydrolytic kinetics of TF_1, dependent on both $[ATP_t]$ and $[Mg_t^{2+}]$. As exhibited at 0.2 mM total Mg^{2+} (Fig. 2A), this inhibition may reach high levels (80–85% of the maximum ATPase activity).

It is noteworthy that the position of the transition between phases I and II is strongly dependent on $[Mg_t^{2+}]$; at 1 mM and 2.5 mM total Mg^{2+}, it takes place at $[ATP_t]$ values close to the $[Mg_t^{2+}]$ value (Fig. 2B,C). The relation of this acceleration phase with the concentrations of the nucleotide and metal cation species will be considered in more detail below.

Theoretical treatment and simulation of the data

A theoretical simulation of the data has to take three main features into account: (1) existence of two distinct

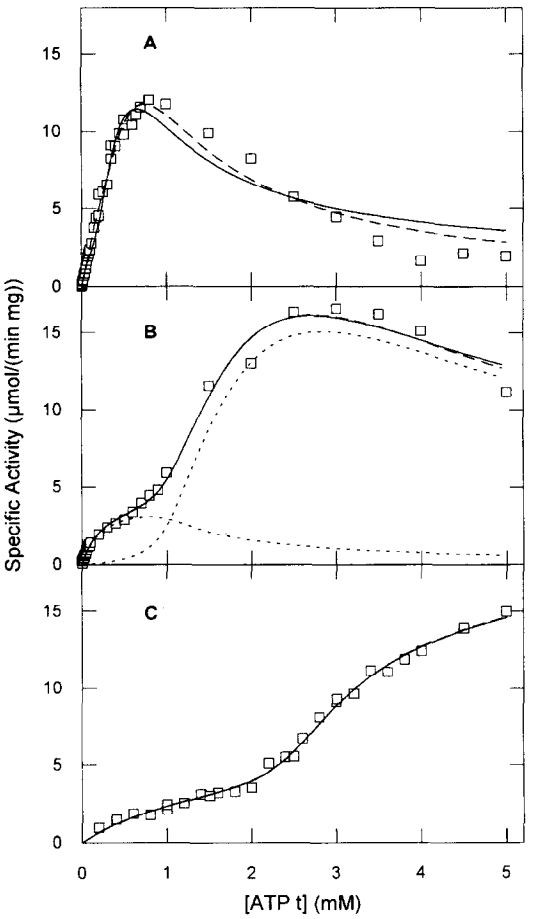

Fig. 2. Influence of total magnesium concentration on specific ATPase activity of TF_1 at 37°C as a function of total ATP concentration. ATPase activities were measured as described under Materials and Methods and in the legend of Fig. 1, in a buffer containing 50 mM Tris-H_2SO_4 (pH 8.0) and 0.2 mM $MgSO_4$ (A), 1.0 mM $MgSO_4$ (B) and 2.5 mM $MgSO_4$ (C). Theoretical curves were calculated as described in detail under Results and data analysis by non-linear fitting to the data of model A (solid lines) and B (dashed lines) (see Ref. [23] and Appendix). The dotted lines in part (B) display the two rates modes which are summed to give the hydrolysis rate predicted by model B. The corresponding optimised Michaelis constants are given in Table 1.

catalytic modes, with different rate levels and different dependences on $[ATP_t]$; (2) at low $[ATP_t]$, apparent inhibition or latency of the high rate catalytic mode displayed in phase II; and (3) inhibition of the ATPase activity at high total ATP concentration.

(1) Predominance of slow rate mode(s) at low total ATP concentration has been reported for F_1-ATPases from various sources [21,36–38]. In most of these studies, it was correlated with single site catalysis (or with operation of only part of the catalytic sites). However, we considered that experimental conditions that are required for observation of single site catalysis (and co-operative acceleration of hydrolysis) were not met in our study (see Discussion).

Then a possible explanation would attribute the two catalytic modes to two distinct independent classes of catalytic sites, with permanently different dependences on the concentrations of the different species, namely free ATP (ATP_f), ATP-Mg and free magnesium (Mg_f^{2+}). The two catalytic modes then would operate in an additive manner over the whole range of $[ATP_t]$.

(2) The mechanism of the apparent initial inhibition of the high rate mode at low $[ATP_t]$ has to be related to the nature of the substrate and to the concentrations of the different species. In the study reported [23], it was shown that both following sets of hypotheses, hydrolysis of ATP-Mg inhibited by Mg_f^{2+}, or hydrolysis of ATP_f after essential activation by Mg_f^{2+}, can account for the apparent inhibition at low $[ATP_t]$ values. On the one hand, according to the classical scheme, the apparent inhibition at low $[ATP_t]$ values would be due to the presence of a high concentration of inhibitory Mg_f^{2+}. This concentration would be drastically lowered when $[ATP_t]$ reaches $[Mg_t^{2+}]$ because of a high degree of Mg^{2+} chelation by ATP. On the other hand, it could be hypothesised that free ATP is the substrate: then the high rate mode of ATP_f hydrolysis would be indirectly inhibited at $[ATP_t] < [Mg_t^{2+}]$ by excess free Mg^{2+}, which displaces the nucleotide-metal chelation equilibrium towards formation of the ATP-Mg complex, at the expense of ATP_f (Fig. 3A). When $[ATP_t]$ increases above $[Mg_t^{2+}]$, $[ATP_f]$ abruptly increases almost as steeply as $[ATP_t]$, and then would allow exhibition of the high rate mode.

(3) As can be seen by comparison of Fig. 2A,B and Fig. 3C, inhibition at high ATP concentration was developed at $[ATP_t]$ levels where [ATP-Mg] was already very close to its asymptotic maximum value, namely $[Mg_t^{2+}]$. Under these conditions the nucleotide species responsible of this inhibition is likely to be ATP_f. Indeed, the classical theory of catalysis by F_1-ATPases attributes inhibition at high $[ATP_t]$ to competitive [19,20] or non-competitive [21] inhibition of ATPase activity by ATP_f. A slightly different mechanism of inhibition at high concentration of free ATP was proposed [23].

Thus, in order to simulate our data, we constructed two catalytic models on the basis of those developed recently [23]. Since we think that we observed multisite steady-state rates in the whole range of $[ATP_t]$, we considered that the kinetic patterns could be theoretically treated using the steady-state assumptions. The two models are derived from the two sets of hypotheses concerning the nature of the substrate and the role of Mg^{2+}: model A is based on the assumption that ATP-Mg is the substrate and that free Mg^{2+} is an inhibitor, while model B is based on the assumption that ATP_f is the substrate and that Mg^{2+} is an essential activator.

In both models, the measured rate was supposed to be, in the whole range of $[ATP_t]$, the sum of two rates, that is the result of the permanent operation of two independent classes of identical catalytic sites. No assumption was made as regards the number of sites in each class. Hydrolysis rates were expressed as functions of free ATP and free

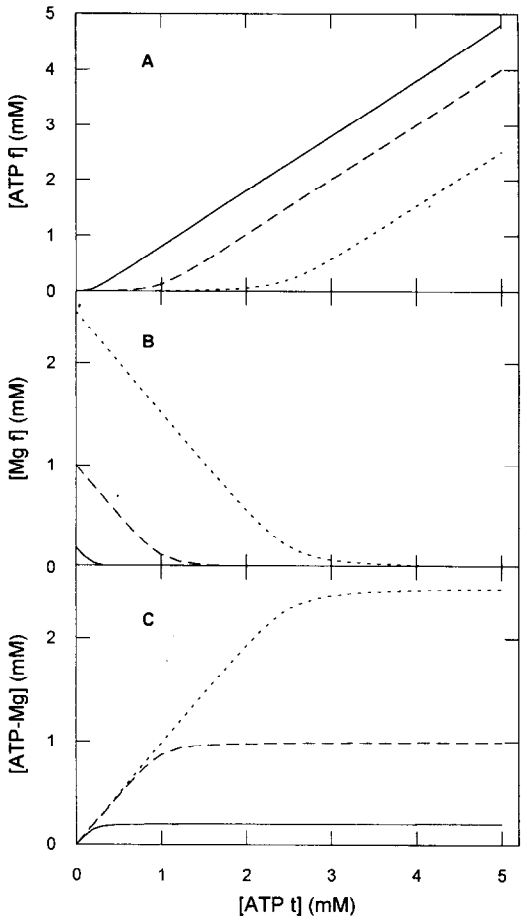

Fig. 3. Theoretical concentrations of free ATP (A), free Mg^{2+} (B) and ATP-Mg complex (C) as functions of total ATP concentration with 0.2 mM total Mg^{2+} (solid lines), 1.0 mM total Mg^{2+} (dashed lines) and 2.5 mM total Mg^{2+} (dotted lines). Theoretical concentrations were calculated assuming a dissociation constant of $1.995 \cdot 10^{-5}$ M for the ATP-Mg complex [18].

magnesium concentrations. These were calculated using the measured dissociation constant for the ATP-Mg complex [18] ($K_{ATP\text{-}Mg} = 1.995 \cdot 10^{-5}$ M). The expressions for the reaction rate corresponding to the two models are given in the Appendix.

We failed to perform a global optimisation, i.e., to simulate satisfactorily all three data sets by a single set of parameters. Therefore, we chose to compare individual fitting results obtained for the different Mg^{2+} concentrations. Numerous sets of initial estimates were tried. Optimisation was assumed to be achieved when variation of the reduced residual quadratic error was lower than 1% between two successive iterations of the optimisation procedure. Criteria of choice among the different sets of optimised parameters were the value of the residual error and the consistency with optimised parameters for the other total Mg^{2+} concentrations.

The values of the Michaelis constants K_1 (slow rate mode) and K_2 (high rate mode) are given in Table 1, and the calculated curves are illustrated by the solid (model A) and the dashed (model B) lines in Fig. 2A, B and C. It is important to notice that large divergences between the two models are observed in the values of K_1 and K_2: each constant is three orders of magnitude lower in model A than in model B.

3.2. Binding of adenine nucleotides to TF_1

Our purpose in studying nucleotide binding to TF_1 was first to cross-check the values of the Michaelis constants that were estimated from the kinetic study. For an enzyme obeying a simple Michaelis-Menten mechanism, the Michaelis constant K_m must be larger than the dissociation constant K_d of the enzyme-substrate complex, and a reliable measurement of K_d might allow the validity of the optimised Michaelis constants to be tested. Our interest was also to check whether the hypothesis of heterogeneity among catalytic sites, which underlay our theoretical approach of kinetic data, could be related to an heterogeneity in binding properties of the different nucleotide binding sites on TF_1. Affinities of TF_1 for nucleotides were esti-

Table 1
Simulation of the kinetics of ATP hydrolysis by TF_1, and ATP binding to native TF_1

	Model A			Model B		
$[Mg_t^{2+}]$ (mM):	0.2	1.0	2.5	0.2	1.0	2.5
K_1	12 ± 13 nM	12 ± 4 nM	64 ± 18 nM	44 ± 5 μM	38 ± 6 μM	7.5 ± 1.4 μM
K_2	7.5 ± 6.8 μM	33 ± 6 μM	43 ± 9 μM	6.1 ± 0.2 mM	4.2 ± 0.1 mM	11.6 ± 0.4 mM
Binding of:		ATP-Mg			Free ATP	
K_d app.		85 ± 27 μM			1.6 ± 0.5 μM	
Number of sites		5.4 ± 0.7			4.9 ± 0.6	

The two models (see Ref. [23] and Appendix) were fitted to the kinetic data from Fig. 2 for each total Mg^{2+} concentration. In model A, ATP-Mg is the substrate, free Mg^{2+} is an inhibitor. In model B, free ATP is the substrate, free Mg^{2+} is an essential activator. In the upper part of the table, the Michaelis constants of the slow rate mode (K_1) and the high rate mode (K_2) are presented for both models and for each total Mg^{2+} concentration. In the lower part of the table, parameters for ATP binding to native TF_1 are given. ATP binding was measured as described in detail under Materials and Methods and in the legend of Fig. 5. Data from Fig. 6 were simulated separately assuming binding of the ATP-Mg chelate and binding of free ATP. Their concentrations were calculated using a dissociation constant of $1.995 \cdot 10^{-5}$ M for ATP-Mg [18]. A single class of independent binding sites was assumed. Kinetic parameters and binding parameters are given ± standard errors.

mated assuming binding of either the nucleotide-Mg^{2+} complex or of free nucleotide.

1.3 ADP per TF_I, bound during incubation in the presence of nucleotide, are not released by extensive dialysis

Although TF_I is free of bound nucleotides after purification, its ability to bind one ADP in a slowly reversible way was reported [15]: such binding properties would disturb measurements of the affinity of TF_I for nucleotide by the method of Hummel and Dreyer. Therefore, it was necessary to characterise the slowly reversible nucleotide binding to TF_I under our conditions.

Prior to this, we measured the nucleotide content of TF_I after its isolation (native TF_I), by acid denaturation of the enzyme and anion-exchange HPLC, as described under Materials and Methods. TF_I was found to contain 0.1–0.2 mol bound ADP per mol TF_I. This value is representative of the endogenous nucleotide content of all native TF_I preparations used in our kinetic studies and nucleotide binding measurements. After incubation of native TF_I in a buffer containing 50 mM Tris-H_2SO_4, 1 mM $MgSO_4$ (pH 8.0) and ADP 1.85-fold more concentrated than TF_I (final ADP concentration $7.24 \cdot 10^{-5}$ M) and thorough dialysis for more than 15 h against the same buffer without ADP, TF_I was found to contain 1.3 mol bound ADP per mol TF_I. This amount of bound ADP could not be reduced by extension of the dialysis to 20 h.

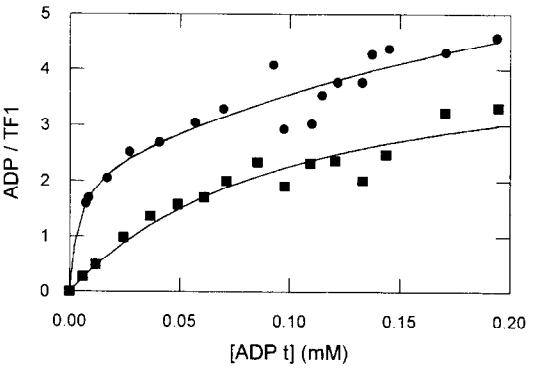

Fig. 4. ADP binding to TF_I as a function of total ADP concentration. ADP binding was measured at room temperature by the method of Hummel and Dreyer [30]. A size exclusion HPLC column (TSK 2000 SW 0.75×30 cm) was equilibrated with a buffer containing 50 mM Tris-H_2SO_4, 1.0 mM $MgSO_4$ (pH 8.0) and the indicated concentrations of ADP. For each ADP concentration, several injections were performed, each one immediately after mixing TF_I (approx. 1 nmol) with a known amount of ADP for internal calibration. ADP binding studies were performed using native TF_I containing 0.17 mol bound ADP per mol TF_I (circles) and TF_I with 1.3 mol bound ADP per mol TF_I (squares) as described in detail under Results and data analysis. Theoretical curves were calculated by non-linear regression assuming two classes of binding sites for native TF_I, and a single class of binding sites for TF_I with 1.3 mol bound ADP per mol TF_I. For the two batches of TF_I, the simulation was separately performed assuming binding of free ADP and binding of ADP-Mg (the resulting calculated curves are superimposed on the plot of ADP binding versus total ADP concentration). Corresponding parameters are given in Table 2.

ADP binding to TF_I

We then studied binding of ADP to TF_I using two different preparations of TF_I. The first set of ADP binding experiments was performed using native TF_I; this enzyme preparation contained 0.17 mol bound ADP per mol TF_I. In the second set of binding experiments, we used TF_I which retained 1.3 mol ADP per mol TF_I after incubation with excess ADP and dialysis against ADP-free buffer (see above). In both cases, 1 mM Mg^{2+} was present at the time of the measurement.

ADP binding to native TF_I was studied by size exclusion HPLC and by anion-exchange HPLC. The data shown in Fig. 4 are from size exclusion experiments only. The two methods gave nearly identical results (data not shown) and thus we estimated that the chromatographic process did not introduce artefacts in the measurement of ADP binding. The binding pattern of ADP to native TF_I as a function of $[ADP_t]$ was clearly biphasic (Fig. 4, upper curve), with an apparent high-affinity component which was already saturated for low total ADP concentrations, and a lower-affinity component which was not yet saturated at the highest total ADP concentration used.

ADP binding to TF_I with 1.3 binding sites previously filled with ADP was studied using size exclusion HPLC. This latter enzyme exhibited quite different binding properties. It is important to note that upon size exclusion HPLC, for zero ADP concentration, 0.3 mol ADP per mol

Table 2
ADP binding to native TF_I and to TF_I containing 1 mol bound ADP per mol TF_I

	Native TF_I		1:1 TF_I:ADP complex	
	number of sites	K_d app.	number of sites	K_d app.
ADP-Mg	2.2 ± 0.4	3.0 ± 2.6 μM	–	–
	7.3 ± 2.4	0.36 ± 0.18 mM	4.6 ± 0.7	95 ± 28 μM
Free ADP	2.2 ± 0.5	0.26 ± 0.22 μM	–	–
	5.6 ± 1.6	23 ± 13 μM	4.2 ± 0.5	6.6 ± 1.7 μM

ADP binding was measured as described in detail under Materials and Methods and in the legend of Fig. 4. Data from Fig. 4 were simulated separately assuming binding of free ADP and binding of the ADP-Mg chelate. Their concentrations were calculated using a dissociation constant of $7.76 \cdot 10^{-5}$ M for ADP-Mg [18]. A single class of independent ADP binding sites was assumed for the 1:1 TF_I-ADP complex, and two classes of independent ADP binding sites were assumed for native TF_I. Binding parameters are given ± standard errors.

TF_1 were released by the enzyme at the moment of injection and migrated with the ADP retention: this resulted in a downward shift of the molar ratio of bound ADP to TF_1 by 0.3 units. The corresponding data which are shown in Fig. 4 (lower curve) were corrected for this effect. Thus, after incubation of native TF_1 with excess ADP, over 1.3 bound ADP which are not released by extensive dialysis, only 1 ADP is retained upon size exclusion HPLC.

The 1:1 TF_1:ADP complex so formed exhibited an apparent monophasic binding pattern (Fig. 4, lower curve): slowly reversible filling of one ADP binding site eliminated the apparent high-affinity binding component which was observed with native TF_1 (Fig. 4, upper curve). Assuming two possible hypotheses, binding of the ADP-Mg complex or binding of free ADP, corresponding dissociation constants were estimated from these data using non-linear regression. The values obtained are shown in Table 2. It should be noted that the estimated values for equilibrium constants are independent on the absolute value of protein concentration and thus are much more reliable than the estimated numbers of sites.

We concluded that one site of native TF_1 is able to bind ADP in a slowly reversible manner at low nucleotide concentrations. The very low rate constant for ADP release from this latter site prevents reliable measurement of its affinity for ADP by classical methods. Subsequent rapidly reversible filling of other ADP binding sites can be described by homogenous affinity for ADP.

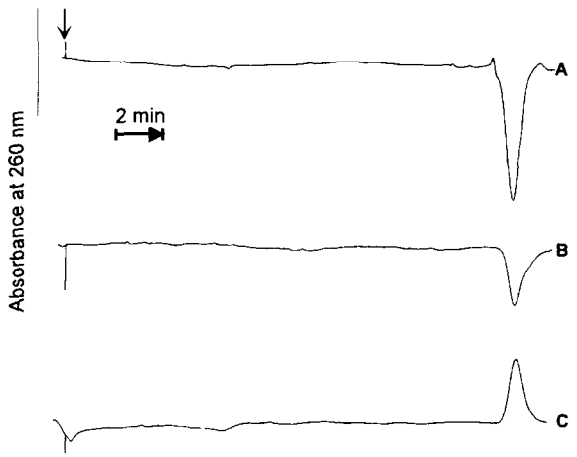

Fig. 5. Typical chromatograms for the measurement of ATP binding to native TF_1. ATP binding was measured at room temperature by the method of Hummel and Dreyer [30], using an anion exchange HPLC column (TSK DEAE 2SW 0.46×25 cm) equilibrated with a buffer containing 50 mM Tris-H_2SO_4, 1 mM $MgSO_4$ (pH 8.0) and, in this example, 58 μM ATP. The baseline corresponds to the absorbance of this buffer at 260 nm. Three successive injections (50 μl) were performed for internal calibration, containing 0.8 nmol TF_1 and for internal calibration either no added ATP (A), 3.7 nmol added ATP (B) and 7.4 nmol added ATP (C). The vertical arrow indicates the injections. Linear regression of the peak area for ATP versus excess of ATP gives, for zero area, the amount of ATP bound to the enzyme at the top of the column at the studied total ATP concentration.

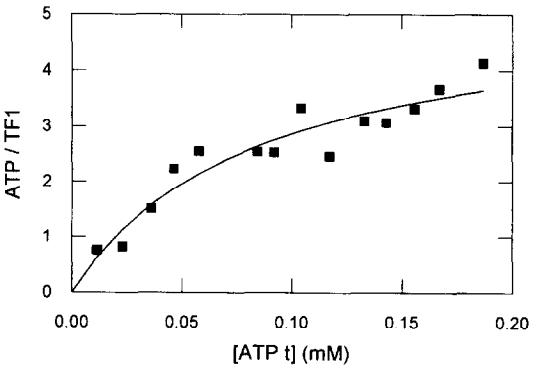

Fig. 6. ATP binding to native TF_1 as a function of total ATP concentration. ATP binding was measured at the indicated total ATP concentrations in a buffer containing 50 mM Tris-H_2SO_4, 1 mM $MgSO_4$ (pH 8.0) as described in the legend of Fig. 5. Theoretical curves were calculated by non-linear regression, assuming a single class of binding sites and either binding of ATP-Mg or binding of free ATP (the resulting curves are superimposed). The corresponding apparent dissociation constants are 85 μM and 1.6 μM, respectively (see Table 1).

ATP binding to TF_1

The affinity of native TF_1 for ATP was measured in the presence of 1 mM Mg^{2+} using an anion-exchange column, which allows ADP and ATP binding to be distinguished. Typical Hummel and Dreyer chromatograms are shown in Fig. 5. Peaks for ATP were reproducible and satisfyingly symmetrical. We therefore considered that this experiment provided a measure of immediate ATP binding to TF_1 at the moment of injection, without influence of ulterior ATP hydrolysis in the column.

ATP binding to native TF_1 as a function of total ATP concentration is shown in Fig. 6. The results can apparently be described assuming a single class of ATP binding sites. The solid line in Fig. 6 is the corresponding calculated saturation curve obtained by non linear fitting of the data, assuming either binding of the ATP-Mg complex or binding of free ATP; corresponding binding parameters are given in Table 1.

4. Discussion

Is the existence of two distinct independent catalytic pathways a reasonable assumption?

Two distinct catalytic modes were identified for the mitochondrial coupling factor [21], and each of them was related to a particular functional state of the enzyme, depending on the presence of bound magnesium at a specific site different from the binding site for the putative substrate ATP-Mg. The two modes were exhibited in two distinct domains of ATP concentration, and hence in two domains of free Mg^{2+} concentration. Thus, these authors interpreted their results assuming a single class of catalytic sites.

Multiphasic plots of ATPase activity versus ATP concentration, which have been shown to be common to F_1-ATPases from various sources [36,38,39], are predicted

by the binding change mechanism. They are usually explained by the existence of co-operative interactions between catalytic sites and by stimulation of the hydrolysis rate at a single catalytic site by progressive operation, at higher substrate concentrations, of the other sites [36,38,40–42]. However, observation of single site catalysis was shown to require the use of substoichiometric substrate concentrations [43]. It was reported that when all the putatively equivalent catalytic sites are operating together, the catalytic behaviour of the enzyme can be satisfyingly described in terms of Michaelis-Menten kinetics [38,39]. Under our conditions, total ATP concentration was always more than three orders of magnitude higher than the enzyme concentration. Therefore, we considered that we only measured rates corresponding to what is generally referred to as multisite catalysis.

In order to account for the existence of two catalytic modes, we assumed the existence of a functional heterogeneity among the catalytic sites. Asymmetry in the properties of catalytic sites seems to be a common feature of all F_1-ATPases [44]. According to the binding change mechanism theory [41], functional asymmetry of equivalent sites during sequential nucleotide binding is due to co-operative interactions between the sites, negative co-operativity of binding and positive co-operativity of catalysis [43,45]. Although this asymmetry is maintained during multisite steady-state catalysis, it is not the result of permanent intrinsic characteristics of particular sites: each new step of substrate binding and products release switches the properties of the different sites in a rotating or alternating manner, in such a way that ATP hydrolysis follows a single catalytic pathway [46]. However, some reports suggest that one catalytic site may keep its original properties even when all other catalytic sites are operating. It was shown [47] that one of the catalytic sites of chloroplast coupling factor reconstituted in liposomes, which is loaded first with ATP under unisite conditions, hydrolyses ATP with a maximal rate of 0.5 s^{-1} when other sites are occupied, whereas other sites catalyse a hydrolysis rate of 80 s^{-1} under the same conditions. A similar observation was made with MF_1 [48]: the promoted turnover rate on the catalytic site loaded first with radioactive ATP was considerably lower than the hydrolysis rate of cold promoter ATP. These results suggest that one catalytic site is permanently different from the others during steady-state ATP hydrolysis.

Kasho et al. [49] studied ATP modulation of oxygen exchange between inorganic phosphate and water during ATP hydrolysis catalysed by TF_1. They found that the distribution of inorganic phosphate isotopomers was best explained by the existence of two catalytic pathways, one of them being characterised by a higher oxygen exchange probability. They proposed that this secondary pathway represents ATP hydrolysis by a less active enzyme form, with a much lower apparent K_m than the major form, and which would constitute a considerable fraction of total enzyme [49]. Another possible hypothesis that is not mentioned by these authors would be the existence of (a) catalytic site(s) permanently different from the others, which would catalyse slow ATP hydrolysis with a low K_m, thus allowing oxygen exchange to occur with high probability.

The results reported here about the binding of one ADP to TF_1 which is resistant to gel filtration HPLC are consistent with the results obtained by Yoshida and Allison [15]. In the latter study, one ADP binding site was identified on β subunits of TF_1, which did not exchange bound ADP with medium nucleotides nor released it upon gel filtration on centrifuge columns. This site was shown to be capable of ATP synthesis in the presence of dimethyl sulfoxide, and hence was proposed to be a catalytic one [15]. Furthermore, it was shown [50] that ADP bound to this site is not released even when all potential ADP binding sites are loaded with ADP, and that release of this ADP requires more than 10^6 catalytic turnovers. This site is likely to be the same as the single high-affinity site on β which is capable of single site hydrolysis of TNP-ATP and which seems not to participate in steady-state catalysis [51]. These results suggest that one catalytic site of TF_1 exhibits unique properties, namely high affinity for adenine nucleotides and low hydrolysis rates, which are conserved even if the other sites are occupied.

Thus, it seems reasonable to assume that distinct classes of catalytic sites can catalyse ATP hydrolysis with different K_m and different rates in the whole range of ATP concentration, in an additive manner. The hypothesis of two classes allows the existence of two catalytic modes to be simply explained and simulated.

The discrepancy between apparently homogenous affinities of the binding sites for the substrate on the one hand (Fig. 6), and discrete heterogeneous kinetic parameters on the other hand is only apparent. Binding affinity is a measure of a thermodynamic equilibrium theoretically independent on time, while kinetic parameters are directly related with the rate constants (k_1, k_{-1} and k_2) of individual reactions of this equilibrium. Furthermore, the value of the rate constant for the hydrolytic reaction (k_2) can result in a large difference between theoretical equilibrium concentration of the enzyme-substrate complex (described by the dissociation constant) and its steady-state concentration (described by the Michaelis constant). Therefore, catalytic sites with similar binding affinities for the substrate may have considerably different values of K_m. Another possibility also exists: one class of ATP binding sites could have been undetectable by the method of Hummel and Dreyer within the overall ATP binding, due to insufficient precision of the data or to a low rate constant of ATP binding.

Nature of the substrate and role of magnesium ions

The interpretation of kinetic studies of ATP hydrolysis by F_1-ATPases [19–22], involving hydrolysis of the ATP-

cation complex and inhibition by the free cation, has become an initial postulate which nowadays underlies all studies on the mechanism of ATP hydrolysis by F_1-ATPases. However, this general agreement was recently questioned [23].

We report here a kinetic study of ATP hydrolysis by TF_1. On the basis of steady-state Michaelis-Menten assumptions (see Ref. [23] and Appendix) and with the hypothesis of existence of two distinct classes of catalytic sites, two models were developed which allowed simulation of the data. Fittings of the data with these two models were equivalent in terms of residual errors (Fig. 2): thus, an important conclusion of this study is that it may be impossible to exclude one model only on the basis of kinetic measurements at different total magnesium concentrations.

Since the concentrations of free ATP and ATP-Mg behave in quite different ways as a function of total ATP concentration, the main divergence between the two models concerned Michaelis constants of the reaction rates. From data about ATP binding to TF_1, dissociation constants could also be measured assuming either binding of ATP-Mg or binding of free ATP. In all cases, Michaelis constants should be larger than the dissociation constant of the enzyme-substrate complex ($K_m = K_d + (k_2/k_1)$). If one assumes binding and hydrolysis of free ATP, both Michaelis constants are significantly larger than the measured dissociation constant (Table 1). If one assumes binding and hydrolysis of ATP-Mg, the estimated Michaelis constant for the slow rate mode (K_1) is two or three orders of magnitude lower than the measured dissociation constant (Table 1), while the Michaelis constant for the high rate mode (K_2) is lower (or of the same order of magnitude). Thus, another important outcome of this study is that comparison between kinetic parameters and dissociation constants advocate the second model, i.e., binding and hydrolysis of free ATP, and essential activation by free magnesium.

The study of the early, transient phases of the time-course of ATP hydrolysis by MF_1 (and submitochondrial particles) in the presence of an ATP regenerating system has given an insight to the role of bound nucleotides. It was shown that the high affinity binding of ADP to F_1 in the presence of Mg^{2+} could transiently inhibit the ATPase activity [52–54]. The inhibitory binding site for MgADP was then proposed to be a catalytic one. As well as endogenous nucleotide, if any, or ADP bound to F_1 upon preincubation, MgADP entrapped at a catalytic site is thought to induce the inhibition, in a time-dependent way, during the course of ATP hydrolysis [55–61]. Moreover, several recent studies suggested that slow binding of ATP to two of the three noncatalytic sites [11,13,62] is able to promote the release of inhibitory MgADP from the catalytic site, and thus to reactivate the enzyme [11,13,14,62,63]. In the case of MF_1, the apparent negative co-operativity of ATP hydrolysis has been recently attributed to this slow binding of ATP to noncatalytic sites [13]. In the case of an enzyme free of bound nucleotides, such as TF_1 or nucleotide-depleted MF_1, the combined influences of nucleotide binding during hydrolysis of low concentrations of ATP result in a triphasic time-course of the reaction [13,63]. Progressive inhibition by MgADP explains, after an initial burst, an intermediate, inhibited phase. Slow binding of ATP to noncatalytic sites then raises the hydrolysis rate up to a final, steady-state level, at the equilibrium between formation of the inhibited F_1-MgADP complex and the ATP-induced release of MgADP.

In this study, we did not observe the triphasic structure of hydrolysis time-course that was described in the case of the same enzyme [63] and of mitochondrial ATPase [13]. The increase of ADP concentration in the reaction medium was a linear function of time and was aligned with the origin, throughout the whole range of ATP concentration. Even though our method would not allow the first tens of seconds to be studied, we should have observed the slow reactivation of the enzyme, according to the time scale described in the case of TF_1 for this phenomenon [63].

Sulfate ions were reported to considerably slow the reactivation process [11,13,63] and to maintain the hydrolysis rate to its value in the intermediate, inhibited phase. Since our measurements were conducted in the presence of millimolar concentrations of sulfate, it could be argued that at low ATP concentrations (i.e., in phase I), the hydrolysis rates that we measured correspond to an inhibited phase stabilised by SO_4^{2-}. Therefore, we checked with 2.5 mM total Mg^{2+} that a total replacement of sulfate by chloride in the reaction medium did not alter either the linearity of hydrolysis time-courses, or the bimodal aspect of the substrate saturation curve as illustrated in Fig. 2C (data not shown). In particular in phase I, identical activity levels were obtained in the presence of sulfate or chloride. Moreover, if the presence of sulfate had been responsible in our conditions of an inhibition of the ATP-dependent reactivation at low ATP concentrations, a qualitative transition in the hydrolysis time-courses should have corresponded to the quantitative transition in the hydrolysis rate as ATP concentration was increased: we did not observe such a qualitative transition. Thus we considered that in the whole range of ATP concentration, the rates that we measured corresponded to the final steady-state rate previously described for ATP hydrolysis [13,63], which was probably attained before the first measurement of ADP concentration. Unfortunately, at the steady-state of ATP hydrolysis, the effects of MgADP-induced inhibition, and the influences of ADP and Mg^{2+} concentrations on the extent of this inhibition are poorly known. A possible mechanism for the steady-state action of Mg^{2+} is tested here (see model A in Appendix and Ref. [23]).

In the case of MF_1, Chernyak and Cross [60] showed that the dissociation of inhibitory MgADP upon dilution of the F_1-MgADP complex down to subnanomolar concentrations was an irreversible process, independent of the pres-

ence of a hundred-fold excess of ADP. They also stated that in the presence of 100 μM ATP, this dissociation was too rapid to be measured by manual techniques. Therefore, since the concentration of TF_1 in our study was 0.4 nM, that is much lower than the concentrations used with the spectrophotometric coupled assay [14,15,53,55,59], it is possible that MgADP dissociation was greatly favored. This would explain a steady state being rapidly attained and this aspect of the hydrolysis time-course not depending on $[ATP_t]$. It is of interest that, in the case of *Escherichia coli* F_1, no indication was obtained for an influence of catalytic-site-bound ADP on unisite ATP hydrolysis or, with physiological ATP concentrations, on the onset of a steady-state rate [64]. However, since numerous kinetic models, distinct from those studied in this work, may be constructed, we cannot fully exclude an alternative interpretation of kinetic data (Fig. 2) which would attribute an inhibitory role to MgADP bound at a catalytic site in the presence of high concentrations of free Mg^{2+}, in particular when $[ATP_t] < [Mg_t^{2+}]$.

Zhou et al. [65] reported a transient burst in the time-course of ATP hydrolysis by CF_1, prior to the setting in of a lower steady-state rate. They attributed this effect to a lag in the onset of Mg^{2+}-induced inhibition of CF_1. Guerrero et al. [66] showed that an increase in free Mg^{2+} concentration lowered the duration of the burst phase, the initial hydrolysis rate, and the steady-state rate. They concluded from those experiments that the delayed inhibition by free Mg^{2+} is due to transitions between active and inactive forms of the enzyme upon slow binding and slow release of Mg^{2+}, and that it requires the presence of enzyme-bound ADP. Hisabori and Mochizuki recently proposed [67] that the inhibitory effect of Mg^{2+} is at least partly due to a Mg^{2+}-induced change in the rate constant for inhibitory ADP binding to CF_1. With TF_1, we did not observe the kinetic sequence described [66], possibly due to the absence of endogenously bound nucleotides on native TF_1. The alignment of the time-courses of ATP hydrolysis with the origin and the rapid onset of a steady-state rate suggest either that an Mg^{2+}-induced inhibition (due to product ADP) did not occur during the course ATP hydrolysis, or that an equilibrium for such an inhibition was reached very rapidly. It should be noted that in the above-mentioned study of the influence of free Mg^{2+} concentration on the ATPase activity [66], ATP-Mg concentration was kept constant. Increasing free Mg^{2+} concentration thus means decreasing free ATP concentration: if free ATP were the substrate of F_1, a decrease of the steady-state rate would also be expected.

In a recent study [68], a relative $[^{32}P]P_i$ release was measured as a function of ATP concentration during hydrolysis of ATP by CF_1 in the presence of Ca^{2+}. The authors observed the existence of a fall, followed by a rise in the initial part of the curve, and concluded that the only possible explanation for that critical pattern is the existence of co-operative interactions between catalytic sites. This would be true only if the ATP-Mg complex is the actual substrate of the enzyme. As a matter of fact, the relative $[^{32}P]P_i$ release is proportional to the ratio of hydrolysis rate to substrate concentration ($v/[ATP]$). It can be shown that a plot of $v/[ATP_t]$ (or $v/[ATP\text{-}Mg]$) versus $[ATP_t]$ (or [ATP-Mg], respectively) would display this pattern of fall and rise in the case of a putative enzyme with independent heterogeneous catalytic sites hydrolysing free ATP with simple Michaelis-Menten kinetics, even if one omits the hypothesis of co-operativity. Thus, another possible explanation of these results [68] would be that CF_1 possesses independent heterogeneous catalytic sites, and that the hydrolysis rate depends on free ATP concentration.

It seems clear from our present results and from others [19–21] that inhibition at high total ATP concentration can be attributed to free ATP. In model A, inhibition by free ATP is assumed to be competitive. In model B, the hydrolysis inhibition at high ATP concentration is attributed to the ineffective partial binding of two molecules of substrate ATP_f to the same catalytic site: each molecule of substrate could interact with a particular sub-site, one with the phosphate binding groups of the site, the other with the adenine binding groups. None of these models, however, is really satisfactory: inhibition by free ATP is probably the results of intricate phenomena, and its elucidation will be necessary for a full comprehension of a fundamental regulatory mechanism of F_1-ATPases.

5. Conclusion

A first element of conclusion which may be drawn from this study is that the existence of two well distinguished steady-state catalytic modes can be explained by the hypothesis that the observed hydrolysis rate is the result of additive operation of two distinct classes of catalytic sites. That hypothesis is consistent with the strong indications which are in favour of a functional heterogeneity of catalytic sites of F_1-ATPases from various sources [47,48,50]. If the existence of two distinct rate modes is actually correlated with the functional heterogeneity of catalytic sites, TF_1 would be a peculiar case among F_1-ATPases. As a matter of fact, the rate of hydrolysis catalysed by the 'low rate' site(s) would be high enough in the case of TF_1 to allow clear distinction from a higher rate mode when activity is measured versus ATP concentration. In the case of other F_1-ATPases, it would be negligible as compared to the rate of catalysis by the 'high rate' sites. Hence, only one catalytic pathway would be generally necessary to explain oxygen exchange patterns [46,69], while a second one is required in the case of TF_1 [49].

In order to simulate the Mg^{2+}-modulated multiphasic patterns which were obtained for the steady-state rate of ATP hydrolysis versus ATP concentration, two simple models were designed. The first one involves hydrolysis of

the ATP-Mg complex and inhibition by Mg^{2+}, the second one involves hydrolysis of free ATP with essential activation by Mg^{2+}. A second element of conclusion is that results of the simulations raise doubts about the ability of purely kinetic experiments to provide conclusive evidences about the nature of the substrate which is hydrolysed by F_1-ATPases and about the actual role of Mg^{2+}.

In an attempt to discriminate between the two models, the affinity of TF_1 for ATP was measured. The purpose of our study is not to discuss what is the precise role of Mg^{2+} during the catalytic events, i.e., the interactions of Mg^{2+} with ATP within the catalytic site. Whatever these interactions may be, what is important to know is the binding sequence of the active species or, in other words, which is the nucleotide concentration that determines the steady-state reaction rate, [ATP_f] or [ATP-Mg]. We think that the latter question had not been answered in a sufficiently unambiguous way. Even if a plausible role of bound inhibitory MgADP cannot be definitely excluded, as for chloroplast F_1 [23], confrontation of estimated kinetic parameters with results concerning ATP binding to TF_1 pleads on behalf of a control of the steady-state reaction rate by free ATP concentration, while Mg^{2+} would be an essential activator of the enzyme.

Acknowledgements

We thank Dr. Francis Haraux and Dr. Philippe Champeil for helpful discussions and Dr. Paul Mathis for critical reading of the manuscript. We also thank PROCOPE, a project for exchange of scientists between France and Germany, sponsored by the Foreign Office of France (MAE) and the German Academic Exchange Service (DAAD), for grants which enabled collaboration between the two laboratories.

Appendix A

The formalism for the calculation of the hydrolysis rate in both models has been developed in Ref. [23]. In model A, ATP-Mg is the substrate, magnesium is an inhibitor. In model B, free ATP is the substrate, magnesium is an essential activator, and the hydrolysis is inhibited by the uneffective binding of two molecules of ATP to the same catalytic site. The following modifications of the models were made. In model A, the inhibition by free ATP is competitive. In both models, the overall hydrolysis rate v is the result of the operation of two independent classes of catalytic sites: v can be written as the sum of two rates with the same expression but with different kinetic parameters.

If 'E' stands for one catalytic site, K_{Mg} is the dissociation constant for the E-Mg complex. K_{ATP} is the dissociation constant of the competitively inhibited E-ATP site (model A) or of the inhibited E-$(ATP)_2$ site (model B). In both models, K_{Mg} and K_{ATP} have the same value in the two terms of the overall rate.

In model A,

$$v = \frac{V_1}{1 + \frac{K_1 K_{ATP-Mg}}{K_{Mg}[ATP]}\left(1 + \frac{K_{Mg}}{[Mg]}\left(1 + \frac{[ATP]}{K_{ATP}}\right)\right)} + \frac{V_2}{1 + \frac{K_2 K_{ATP-Mg}}{K_{Mg}[ATP]}\left(1 + \frac{K_{Mg}}{[Mg]}\left(1 + \frac{[ATP]}{K_{ATP}}\right)\right)}$$

In model B,

$$v = \frac{V_1}{1 + \frac{K_1}{[ATP]}\left(1 + \frac{K_{Mg}}{[Mg]}\right) + \frac{[ATP]}{K_{ATP}}} + \frac{V_2}{1 + \frac{K_2}{[ATP]}\left(1 + \frac{K_{Mg}}{[Mg]}\right) + \frac{[ATP]}{K_{ATP}}}$$

where K_1 (K_2) and V_1 (V_2) are the K_m and V_m values of the sites of the first (second) class, $K_{ATP\text{-}Mg}$ is the dissociation constant of the ATP-Mg chelate.

References

[1] Futai, M., Noumi, T. and Maeda, M. (1989) Annu. Rev. Biochem. 58, 111–136.
[2] Senior, A.E. (1990) Annu. Rev. Biophys. Biophys. Chem. 19, 7–41.
[3] Cross, R.L. (1992) in Molecular Mechanisms in Bioenergetics (Ernster, L., ed.), pp. 317–330, Elsevier, Amsterdam.
[4] Bianchet, M., Ysern, X., Hullihen, J., Pedersen, P.L. and Amzel, M.L. (1991) J. Biol. Chem. 266, 21197–21201.
[5] Abrahams, J.P., Leslie, A.G.W., Lutter, R. and Walker, J.E. (1994) Nature 370, 621–628.
[6] Cross, R.L. and Nalin, C.M. (1982) J. Biol. Chem. 257, 2874–2881.
[7] Wise, J.G., Duncan, T.M., Latchney, L.R., Cox, D.N. and Senior, A.E. (1983) Biochem. J. 215, 343–350.
[8] Girault, G., Berger, G., Galmiche, J.M. and André, F. (1988) J. Biol. Chem. 263, 14690–14695.
[9] Perlin, D.S., Latchney, L.R., Wise, J.G. and Senior, A.E. (1984) Biochemistry 23, 4998–5003.
[10] Issartel, J.-P., Lunardi, J. and Vignais, P.V. (1986) J. Biol. Chem. 261, 895–901.
[11] Milgrom, Y.M., Ehler, L.L. and Boyer, P.D. (1990) J. Biol. Chem. 265, 18725–18728.
[12] Murataliev, M.B. (1992) Biochemistry 31, 12885–12892.
[13] Jault, J.-M. and Allison, W.S. (1993) J. Biol. Chem. 268, 1558–1566.
[14] Milgrom, Y.M. and Cross, R.L. (1993) J. Biol. Chem. 268, 23179–23185.
[15] Yoshida, M. and Allison, W.S. (1986) J. Biol. Chem. 261, 5714–5721.
[16] Feldman, R.I. and Sigman, D.S. (1982) J. Biol. Chem. 257, 1676–1683.
[17] Sakamoto, J. and Tonomura, Y. (1983) J. Biochem. 93, 1601–1614.
[18] Pecoraro, V.L., Hermes, J.D. and Cleland, W.W. (1984) Biochemistry 23, 5262–5271.
[19] Ulrich, F. (1964) J. Biol. Chem. 239, 3532–3536.

[20] Hochman, Y., Lanir, A. and Carmeli, C. (1976) FEBS Lett. 61, 255–259.
[21] Adolfsen, R. and Moudrianakis, E.N. (1978) J. Biol. Chem. 253, 4380–4388.
[22] Anthon, G.E. and Jagendorf, A.T. (1983) Biochim. Biophys. Acta 723, 358–365.
[23] Berger, G., Girault, G., Galmiche, J.M. and Pezennec, S. (1994) J. Bioenerg. Biomembr. 26, 335–346.
[24] Ohta, S., Tsuboi, M., Oshima, T., Yoshida, M. and Kagawa, Y. (1980) J. Biochem. 87, 1609–1617.
[25] Kagawa, Y and Yoshida, M. (1979) Methods Enzymol. 55, 781–787.
[26] Berger, G., Girault, G. and Galmiche, J.M. (1990) J. Liquid Chrom. 13, 4067–4080.
[27] Berger, G., Girault, G., André, F. and Galmiche, J.M. (1987) J. Liquid Chrom. 10, 1507–1517.
[28] Bradford, M. (1976) Anal. Biochem. 72, 248–254.
[29] Ohta, S., Yohda, M., Ishizuka, M., Hirata, H., Hamamoto, T., Otawara-Hamamoto, Y., Matsuda, K. and Kagawa, Y. (1988) Biochim. Biophys. Acta 933, 141–155.
[30] Hummel, J. and Dreyer, W. (1962) Biochim. Biophys. Acta 63, 530–532.
[31] Berger, G., Girault, G. and Galmiche, J.M. (1989) J. Liquid Chrom. 12, 535–551.
[32] Scatchard, G. (1949) Ann. N.Y. Acad. Sci. 51, 660–672.
[33] Penefsky, H.S. (1977) J. Biol. Chem. 252, 2891–2899.
[34] Pullman, M., Penefsky, H.S., Datta, A. and Racker, E. (1960) J. Biol. Chem. 235, 3322–3329.
[35] Norby, J.G. (1970) Acta Chem. Scand. 24, 3276–3286.
[36] Wong, S.-Y, Matsuno-Yagi, A. and Hatefi, Y. (1984) Biochemistry 23, 5004–5009.
[37] Harris, D.A. (1989) Biochim. Biophys. Acta 974, 156–162.
[38] Labahn, A. and Gräber, P. (1993) Biochim. Biophys. Acta 1141, 288–296.
[39] Andralojc, P.J. and Harris, D.A. (1990) Biochim. Biophys. Acta 1016, 55–62.
[40] Berden, J.A., Hartog, A.F. and Edel, C.M. (1991) Biochim. Biophys. Acta 1057, 151–156.
[41] Gresser, M.J., Myers, J.A. and Boyer, P.D. (1982) J. Biol. Chem. 257, 12030–12038.
[42] Cross, R.L. (1988) J. Bioenerg. Biomembr. 20, 395–405.
[43] Grubmeyer, C., Cross, R.L. and Penefsky, H.S. (1982) J. Biol. Chem. 257, 12092–12100.
[44] Amzel, L.M., Bianchet, M.A. and Pedersen, P.L. (1992) J. Bioenerg. Biomembr. 24, 429–433.
[45] Cross, R.L., Grubmeyer, C. and Penefsky, H.S. (1982) J. Biol. Chem. 257, 12101–12105.
[46] Hutton, R.L. and Boyer, P.D. (1979) J. Biol. Chem. 254, 9990–9993.
[47] Fromme, P. and Gräber, P. (1989) FEBS Lett. 259, 33–36.
[48] Bullough, D.A., Verburg, J.G., Yoshida, M. and Allison, W.S. (1987) J. Biol. Chem. 262, 11675–11683.
[49] Kasho, V.N., Yoshida, M. and Boyer, P.D. (1989) Biochemistry 28, 6949–6954.
[50] Hisabori, T., Kobayashi, H., Kaibara, C. and Yoshida, M. (1994) J. Biochem. 115, 497–501.
[51] Hisabori, T., Muneyuki, E., Odaka, M., Yokoyama, K., Mochizuki, K. and Yoshida, M. (1992) J. Biol. Chem. 267, 4551–4556.
[52] Fitin, A.F., Vasilyeva, E.A. and Vinogradov, A.D. (1979) Biochem. Biophys. Res. Commun. 86, 434–439.
[53] Minkov, I.B., Fitin, A.F., Vasilyeva, E.A. and Vinogradov, A.D. (1979) Biochem. Biophys. Res. Commun. 89, 1300–1306.
[54] Vasilyeva, E.A., Fitin, A.F., Minkov, I.B. and Vinogradov, A.D. (1980) Biochem. J. 188, 807–815.
[55] Vasilyeva, E.A., Minkov, I.B., Fitin, A.F. and Vinogradov, A.D. (1982) Biochem. J. 202, 9–14.
[56] Vasilyeva, E.A., Minkov, I.B., Fitin, A.F. and Vinogradov, A.D. (1982) Biochem. J. 202, 15–23.
[57] Feldman, R.I. and Boyer, P.D. (1985) J. Biol. Chem. 260, 13088–13094.
[58] Drobinskaya, I.Ye., Kozlov, I.A., Murataliev, M.B. and Vulfson, E.N. (1985) FEBS Lett. 182, 419–424.
[59] Milgrom, Y.M. and Boyer, P.D. (1990) Biochim. Biophys. Acta 1020, 43–48.
[60] Chernyak, B.V. and Cross, R.L. (1992) Arch. Biochem. Biophys. 295, 247–252.
[61] Hyndman, D.J., Milgrom, Y.M., Bramhall, E.A. and Cross, R.L. (1994) J. Biol. Chem. 269, 28871–28877.
[62] Milgrom, Y.M., Ehler, L.L. and Boyer, P.D. (1991) J. Biol. Chem. 266, 11551–11558.
[63] Paik, S.R., Jault, J.-M. and Allison, W.S. (1994) Biochemistry 33, 126–133.
[64] Senior, A.E., Lee, R.S.F., Al-Shawi, M.K. and Weber, J. (1992) Arch. Biochem. Biophys. 297, 340–344.
[65] Zhou, J.-M., Xue, Z., Du, Z., Melese, T. and Boyer, P.D. (1988) Biochemistry 27, 5129–5135.
[66] Guerrero, K., Xue, Z. and Boyer, P.D. (1990) J. Biol. Chem. 265, 16280–16287.
[67] Hisabori, T. and Mochizuki, K. (1993) J. Biochem. 114, 808–812.
[68] Andralojc, P.J. and Harris, D.A. (1994) Biochim. Biophys. Acta 1184, 54–64.
[69] Kohlbrenner, W.E. and Boyer, P.D. (1983) J. Biol. Chem. 258, 10881–10886.